An algorithm to automate the filtering and classifying of 2D LiDAR data for site-specific estimations of canopy height and width in vineyards

Anice Cheraiet, Olivier Naud, Mathilde Carra, Sébastien Codis, Frédéric Lebeau, James Taylor

An algorithm to automate the filtering and classifying of 2D LiDAR data for site-specific estimations of canopy height and width in vineyards

A. Cheraiet[a, b, *], O. Naud[a], M. Carra[a], S. Codis[b], F. Lebeau[a,c] and J.A. Taylor[a].
[a]ITAP, INRAE, Montpellier SupAgro, University of Montpellier, 361 rue Jean-François Breton, 34000 Montpellier, France
[b]IFV French Vine and Wine Institute, 3430 Route de l'Espiguette, 30240 Le Grau-du-Roi, France
[c]Biosystems Dynamics and Exchanges (BioDynE), TERRA Teaching and Research Center, Gembloux Agro-Bio Tech, University of Liege, Gembloux, Belgium
*Correspondence: anice.cheraiet@vignevin.com

Abstract

The 3D characterisation of individual vine canopies with a LiDAR sensor requires point cloud classification. A Bayesian point cloud classification algorithm (BPCC) is proposed that combines an automatic filtering method (AFM) and a classification method based on clustering to process LiDAR data. Data were collected on several grape varieties with two different modes of training. To evaluate the quality of the BPCC algorithm and its influence on the estimation of canopy parameters (height and width), it was compared to an expert manual method and to an established semi-automatic research method requiring interactive pre-treatment (PROTOLIDAR). The results showed that the AFM filtering was similar to the expert manual method and retained on average 9% more points than the PROTOLIDAR method over the whole growing season. Estimates of vegetation height and width that were obtained from classification of the AFM-filtered LiDAR data were strongly correlated with estimates made by the PROTOLIDAR method (R^2 = 0.94 and 0.89, respectively). The classification algorithm was most effective if its parameters were permitted to be variable through the season. Optimal values for classification parameters were established for both height and width at different phenological stages. On the whole, the results demonstrated that although the BPCC algorithm operates at a higher level of automation than PROTOLIDAR, the estimates of canopy dimensions in the vineyards were equivalent. BPCC enables the possibility to adjust the spray rate according to local vegetative characteristics in an automated way.

Key words

Ground-based 3D LiDAR, Point clouds partition, Automatic filtration, Canopy dimensions, Variable rate, Crop protection.

Nomenclature

AFM	automatic filtering method
BBCH	describes the phenological development of grapes using the BBCH-scale
BPCC	Bayesian point cloud classification
CCC	correlation coefficient of concordance
CMM	conventional manual measurements
CV-RMSE	coefficient of variation of root mean square error, %
D	distance between the LiDAR travel line and the Line of Trunk, m
D_ε	distance indicative of the angle range (ε) of LiDAR beams intercepted by the ground in the grassed zone, m
D_δ	distance indicative of the angle range (δ) of LiDAR beams intercepted by the ground in the inter-row, m
HEF	human expert filtration
HG	height of grassed zone above ground, m
HS	height of the LiDAR above ground, m

Hsc	height of the start of canopy growth above the ground, m
H_ε	distance defined along the y-axis between the LiDAR emission point and the first (closest) 5% beams intercepted in the grassed zone, m
LiDAR	light detection and ranging
LoT	line of trunks
PPP	plant protection products
vine unit	the area of foliage corresponding to 0.5 m before and after the vine trunk; signifies a standardised individual vine
VH	vegetation height, m
VW	vegetation width, m
β_H	adjustable threshold during the season defined to estimate VH
β_w	adjustable threshold during the season defined to estimate VW
ΔW	distance interval between two consecutive vertical scans, m
$\Delta\theta$	$\Delta\theta$ angular resolution of the scans, degree
θ	angular resolution of the scans, degree
μ	population mean of the points along the y or z axis, m
ρ	radial distance, m
σ	standard deviations of the points along the y or z axis, m
δ	angle range where the LiDAR beams are removed as intercepted by the ground in the inter-row, in degrees
ε	angle range where the LiDAR beams are removed as intercepted in the grassed zone, in degrees

1. Introduction

Over the past two decades, various advances towards more precise and efficient spray systems have been proposed for different crops, including vineyards (Siegfried et al., 2007; Walklate & Cross., 2013). Although these advances differ in their assumptions and calculations, most of them are based on a characterisation of the canopy. The important factors to consider to ensure an efficient spray application process are the geometric characteristics of the canopy (Solanelles et al., 2006; Llorens et al., 2011a) and the relationship between the quantity of plant protection products (PPP) sprayed and the deposits obtained on the foliage, expressed as a quantity per surface area of organs to protect (Gil et al., 2014). As stated by Gil et al. (2013), the risk levels to harm sensitive non-target areas during the spray application process are related to dose rates and will depend on both the total amount of PPP sprayed and the spraying efficiency over the entire canopy. It has been stated that correctly targeting and adjusting deposition to canopy dimensions/structure will lead to a considerable increase in the efficiency of applications (Vercruysse et al., 1999; Gil et al., 2007), thereby reducing the total amount of PPP required in accordance with EU objectives (Llorens et al., 2010). This has led to the development of variable rate spraying technologies and methodologies (Gil et al., 2013). These techniques hypothesise that foliar application should target similar deposits per quantity of vegetation to be protected, regardless of the canopy shape or density. In this context, the development of precision spraying technologies that take into account the dimensional characteristics of the canopy to regulate nozzle flow is one of the levers that has been identified to reduce PPPs in perennial crops (Berk et al., 2016).

Canopy dimensions can be retrieved manually (Viret et al., 2005; Rosell Polo et al., 2009) or obtained from sensor measurements (Rosell et al., 2012). Manual measurements are time-consuming and have limited suitability under production conditions. Using them requires an extrapolation of measurements from a few locations across the entire field, which generally implies some assumptions about the

homogeneity of crop characteristics within a production system. This disregards the knowledge that canopy size exhibits spatial variation in vineyard blocks (Tisseyre et al., 2008; Taylor et al., 2013). In order to increase spatial resolution to account for known variability in canopy size, vineyard canopy structure can be indirectly estimated using various types of sensors. The literature includes numerous studies that have characterised vine dimensions from the scale of the estate to the individual vine (Rosell et al., 2012; Arnó et al., 2017). Sensors used to date include ultrasonic sensors (Gil et al., 2007; Llorens et al., 2011a), stereo vision imagery (Andersen et al., 2005) including unmanned aerial vehicle (UAV) mounted photogrammetry (Mathews et al., 2013; Miranda et al., 2017; de Castro et al., 2018) and 2D terrestrial Laser imaging Detection And Ranging (LiDAR) sensors (Poni et al., 1996; Rosell Polo et al., 2009; Siebers et al., 2018).

The use of laser sensors to digitise the 3D features (or characteristics) of crops (particularly in viticulture) has been established for some decades but is still mainly limited to the research domain. An early attempt to use laser scanning in viticulture was the study by Poni et al. (1996), who used a 2D LiDAR mounted on an arc-shaped structure to simply calculate the light interception of each vine organ (leaves, trunk, cordon etc…). Since this initial work, interest and development in the use of LiDAR in vineyards has increased and it is becoming more frequently used to non-destructively characterise vegetation structure, shape and biomass (Colaço et al., 2018; Jaakkola et al., 2010). Using LiDAR sensing to measures distances from the sensor to a target over a plane, has a particular interest for the real-time determination of canopy structure during spray operations. 3D scanning is possible when a 2D LiDAR is deployed on a moving platform (Rovira-Más et al., 2006) with a well-determined method of geo-referencing the LiDAR data. Canopy characterisation using 2D LiDAR has been proposed in vineyard studies (Palacin et al., 2007; Sanz et al., 2018) and 3D point clouds have been used to digitally reconstruct and describe the geometric characteristics of vegetation cover with a high level of accuracy (Moorthy et al., 2011). A system developed by Rosell et al. (2012) made it possible to obtain 3D digitised point clouds of crops, from which a large amount of information, such as height, width, volume, leaf area index and leaf area density, could be obtained for a plant or an area of the crop. Arnó et al. (2013) concluded that LiDAR systems were able to measure the geometric characteristics of plants with sufficient precision for most site-specific agriculture applications.

For high-resolution canopy characterisation, LiDAR systems have an advantage over ultrasonic and stereoscopic imagery approaches because of their ability to provide information on both canopy dimensions and density. Ultrasonic sensors were used before LiDAR systems became affordable and available (Schumann et al., 2005), but did not gain widespread popularity. This was due to issues regarding the large angle of divergence of the wave beams (which limits the resolution and accuracy of the measurements) (Stajnko et al., 2012), the need for multiple sensors to cover vine and tree crops (Lee et al., 2009) and limitations with the proximity to the crop at which the sensor can be effectively deployed (Llorens et al., 2011a). Recent advances in UAV-based photogrammetry have indicated a high potential for their use in mapping canopy shape (de Castro et al., 2018). However, mapping canopy density with stereoscopy is still an issue (Torres-Sánchez et al., 2018), and this is critical for modelling spray deposition and adjusting sprayer operation (Campos et al., 2019). Moreover, UAV-based sensors are also not suitable for real-time applications and require a pre-application survey combined with a prescription mapping approach. While LiDAR systems could equally be used pre-spraying to develop prescription spray maps, they also have the potential to be used in front of a sprayer to generate on-the-go, real-time 3D information for variable-rate spraying (Llorens et al., 2010). In the latter real-time use-case for LiDAR, robust and rapid data processing methods will be required to ensure that correct information is transferred to the spray control system.

The literature presents different types of vegetative indicators, such as the tree row volume (TRV) (Byers et al., 1971; Sanz et al., 2013) and the leaf wall area (LWA), which can be used to characterise vegetation structure from canopy dimensions. These are measured either manually or with sensors. There are high resolution variants of the LWA, such as the pixelated leaf wall area (PLWA) (del-Moral-Martínez et al., 2015) and the leaf wall area by points (LWApts) proposed by Bastianelli et al. (2017). When LWA is constant, PLWA and LWApts may exhibit variations due to changes in canopy density. The tree area index (TAI) (Walklate et al., 2002) is based on the notion of light interception and integrates both canopy density and variations of geometry surface area density (SAD) (Schultz, 1995). All of these vegetative indicators aim to simplify the complex structure of vegetation by describing it as a simple geometrical form, sometimes with a feature representing density. However, before these indicators can be calculated from sensor-based data, different processes are required to obtain the primary canopy dimensions from these data.

The first challenge is to obtain a complete 3D point cloud of the entire canopy. Typically, this has required the merging of data collected from the left and right sides of the vineyard (or orchard) row at potentially different times, i.e. during different transects (Sanz et al., 2004). Various tedious and difficult methodologies have been proposed, such as placing reference elements at specific points in the row that can be identified within the canopy point cloud. This complicates data management (Rosell et al., 2009; Sanz et al., 2013). Subsequently, other developments have improved this process with the coupling of global navigation satellite system (GNSS) positioning (Llorens et al., 2011b; Escolà et al., 2017) and inertial measurement units (IMUs) (del-Moral-Martínez et al., 2016). However, GNSS and IMUs both require high quality, expensive specialised equipment. This increases the cost and the processing required and affects the transferability of the research methods into commercial applications. Furthermore, obtaining scans of both sides of the canopy requires sensors to be deployed in every vineyard row. While this has been possible to date in research-based studies, the reality of agricultural practices is that vineyard traffic is usually only every second or third row depending on equipment configuration. It is more likely that only one side of the canopy (a half-canopy scan) will be sensed during any single vineyard operation. This remains problematic, as approaches to estimate canopy dimensions from 'half-canopy' (one-side) LiDAR scans, and their accuracy, have not yet been well-developed.

The second challenge is the filtering procedure of the 3D point cloud. Given the large number of beams emitted by a 2D LiDAR, the selection and classification of "points of interest" becomes an important pre-processing task before canopy dimensions and vegetative indicators can be calculated. A significant number of points are intercepted in regions that are not relevant for the calculation of vegetative indicators, such as the ground, grassed areas, the vine trunk, adjacent rows or the trellis wires (Bastianelli et al., 2017). However, in the available literature on applications of mobile 2D LiDAR in vineyards and orchards, there are very limited explanations and details on the procedures for filtering 3D point clouds. In many studies, the goal was to establish the proof of concept and the data filtering was performed with intensive human intervention (Palacin et al., 2007; Rinaldi et al., 2013). This laborious human intervention at the pre-processing step is not practical if LiDAR is to be deployed in production contexts. Rapid, repeatable, robust filtering methods are needed to ensure the correct estimation of simple vegetative parameters, such as vegetation height or width. These methods need to be effective at all stages of canopy development, from small open canopies during early shoot development to large, potentially dense canopies late in the season. Research methods developed and used to date have tended to focus on filtering and pre-processing data obtained at specific growth stages, not collectively across all growth stages. If LiDAR, or any other sensing technology, is to be successfully incorporated into variable-rate PPP spraying regimes, the technology must be effective

across a wide range of canopy sizes and adaptable to changing canopy conditions. Arguably, the most important period for applying PPP is when the canopy size and shape is rapidly developing during early to mid-season shoot growth. The need for rapid and robust filtering of these large 3D datasets will become even more critical when real-time processing is required for on-the-go applications in spatially variable canopy systems.

The research presented here aims to address these issues of half-canopy scans and an evolving canopy structure by proposing and testing a novel method for the automated pre-processing and filtering of LiDAR data. The method was designed to remain effective as canopy size and shape change quickly through the first half of the growing season and to be applicable in commercial agricultural situations. The specific objectives of this work were to:
(1) propose an adaptable algorithm that applies an automatic filtering method to remove artefacts and non-vine data from 2D LiDAR data collected from only one side of the vine canopy, and then classifies and separates the canopy zone from other vine components (trunk, vegetation, trellis wires) without any operator intervention,
(2) use the proposed algorithm to estimate canopy height and width from LiDAR surveys in several vineyard blocks in southern France and,
(3) assess the quality of these estimations of canopy dimensions by comparing them to canopy dimensions derived from an existing standard LiDAR data filtering method, which is not automated and requires human intervention, and to conventional manual canopy measurements.

2. Materials and methods

2.1. Fields trials

A vineyard with four different blocks ("Les pins", "Aglae", "Terre blanche" and "Franquet") of four different varieties of *Vitis vinifera* L. cv (Marselan, Cabernet Sauvignon, Chardonnay and Petit Verdot), with contrasting vigour, was chosen for the study in 2019. Located in Grabels, close to Montpellier (Hérault, France), the study vineyard is characteristic of a vineyard from the south of France, both in terms of grape varieties and training systems. The rows were north-south oriented for "Les pins", and northeast-southwest for "Aglae", "Terre blanche" and "Franquet". Two different training systems were used: Royat cordon for "Les pins", "Aglae" and "Franquet" and Guyot for "Terre Blanche". Vines were trained (one carrying wire and one trellising wire) in all blocks. Rows were separated by distance D_{ir}, with D_{ir} equal to 2.5 m in all blocks and vine spacing in the row was 1 m. For each block, 20 vines were selected and their trunks geolocated with a LEICA Viva GS10 dual-frequency GNSS receiver equipped with a Siemens MC75 GSM/GPRS individual module, triple-frequency antennas (GPS/GLONASS/Galileo) LEICA AS10 and CS10 radio controls. The same vines were followed throughout the season. 2D LiDAR and manual characterisation of vegetation were carried out on seven dates during the season (T1: 2019/04/29, T2: 2019/05/13, T3: 2019/05/21, T4: 2019/05/28, T5: 2019/06/20, T6: 2019/07/18, T7: 2019/07/31). These dates correspond respectively to the following BBCH scale growth stages (Lorenz et al., 1994): three leaves spread out (14), four to six leaves spread out (53), separate flower buds (57), beginning of flowering (61), flowering (70), berry development (76), bunch closure (81).

2.2. Measurement system

2.2.1. Conventional manual measurement (CMM)

Two different canopy parameters were manually measured at each vine: canopy height (m) and canopy width (m). Manual observations were performed according to the protocol of Manktelow and Praat (1997). Briefly, canopy height was defined from the first leaf above the trunk to the highest leaf in the canopy in the area above the vine trunk. For canopy width, the canopy zone was divided into

three equal vertical sections and a measurement made horizontally in each section between the external canopy leaves with a 2 m ruler. The three measurements were averaged to give the mean canopy width. Each measurement aimed to include > 99 % of the canopy (i.e. some protruding branches were ignored).

2.2.2. LiDAR sensor specifications

Data acquisition unit

A Sick LMS100 (SICK AG, Düsseldorf, Germany) 2D LiDAR sensor was used in the study. The LMS100 LiDAR is a fully-automatic divergent laser scanner based on time-of-flight (TOF) measurement with a systematic error of ± 30 mm, a selectable angular resolution ($\Delta\theta$) set to 0.5° and a range of 270°.With these settings, there were 541 distances (ρ, from the sensor to the interception point) that corresponded to one complete laser mirror rotation. This set of 541 distances is called a "scan" throughout the article and scans were repeated at 50 Hz. The Sick LMS100 laser emission wavelength is 905 nm (near infrared) and it is Class one eye-safe. This sensor was coupled to a Real Time Kinematic (RTK) GNSS receiver (Teria GSM correction, Vitry-sur-Seine, France) and an Effibox data acquisition unit (Effidence society, Romagnat, France) that was used as a data-logger. After surveys, the data were transferred to a laptop over a Wi-Fi network. The sensors were mounted on a dedicated stainless-steel mast placed behind a tractor according to a previously described procedure (Bastianelli et al., 2017) at a height ranging from 1.0 m to 1.40 m above the ground level (HS). Height was adjusted up during the season to account for increasing canopy height (Figure 1A). Collectively the sensors and mobile equipment provided a 3D measurement system.

The tractor was driven along the vineyard rows at a constant forward travel speed (FTS) (Figure 1B) of 5 km h^{-1}, with a systematic error of ± 0.21 km h^{-1} (IFV, internal report, October, 2018). The 20 target vines were located in various locations along the vineyard rows. The RTK-GNSS was used to identify the starting point of these 20 target vines, after which the scans were aggregated, using a fixed forward distance based on the constant tractor speed, to generate a 3D point cloud reconstruction of the vine environment (Figure 1B). During the trials, only one side of the canopy was scanned for each vineyard row.

2.3. Vine unit local 3D point cloud construction

A vine unit, corresponding to an individual vine, was defined according to the direction of travel (x), considering 0.5 m before and 0.5 m after the vine trunk centre (Figure 1B). Vertical scans of the vine canopy were obtained from the 2D LiDAR. Each scan was composed of distances between the LiDAR and objects in the path of the laser beam. The coordinate system origin (O) was defined as the first position of the 2D LiDAR during the measurement on the studied vine unit. The time stamp *t* (in seconds) was given by the Effibox acquisition unit. The distance interval between two consecutive vertical scans (ΔW) was 0.028 m along the direction of travel of the tractor (Figure 1B). For each point of the cloud, the x coordinate was calculated by multiplying *t* by the travel speed. The y and z coordinates (informing on canopy height and width respectively) were obtained by a polar (ρ, θ) (Figure 1A) to Cartesian (y, z) coordinates transformation. Therefore, the 3D point cloud of the vine unit was generated within a Cartesian coordinate system.

Figure 1 near here

2.4. Filter algorithms and LiDAR data analysis

In this section, the methodologies of the two approaches to be compared are presented. The first, PROTOLIDAR, is considered here as a standard approach. It requires human intervention and is based on work by Rinaldi et al. (2013). The second is the novel algorithm BPCC.

2.4.1. PROTOLIDAR methodology

The data files were analysed using the open source statistical software R (Version 1.2.5001) (R Development Core Team, 2019) and the PROTOLIDAR package (PROcess TO LIDAR Data) (Rinaldi et al., 2013). PROTOLIDAR contains three functions to characterise the vine canopy (height, width and front view) from the LiDAR point cloud. The tool performs statistical analysis on the outputs and estimates the leaf area index (LAI), LWA and TRV. For the pre-processing (filtering), the methodology described in Rinaldi et al. (2013) was used. The 3D point cloud was trimmed using the Extract_plant_grapevine function with manually defined thresholds, leaving only the area of interest (i.e. the canopy). This function removed areas of the 3D point cloud that were not associated with the canopy, including LiDAR returns from ground and under vine weeds as well as vines in neighbouring rows.

Once the data had been filtered to a canopy-only response, the PROTOLIDAR package allowed user-defined parameters to be set to characterise the vegetation. The functions Width_canopy and Height_canopy permit the characterisation of vegetation height (VH) and vegetation width (VW) respectively. The minimum possible height was defined manually as the cordon height. VH was estimated from the lowest registered point of canopy LiDAR returns above the defined cordon height (denoted as Height start canopy (Hsc)) to the highest registered point of canopy returns along the y-axis. VW was estimated using the same methodology as for VH, but by considering points along the z-axis.

2.4.2. LiDAR Bayesian point cloud classification algorithm (BPCC)

The BPCC is a 2-stage algorithm. It comprises an automatic filter to remove points of non-interest and a hierarchical cluster-based method to derive canopy dimensions. The two stages are presented in their respective subsections.

2.4.2.1. Automatic filter method (AFM)

As the 2D LiDAR sensor scans the entire vineyard, not just the vine canopy, points that belong to the canopy must be automatically identified and distinguished from points associated with other elements (ground, non-vine vegetation, etc…). This pre-processing is critical to estimate canopy dimensions (height and width) as accurately as possible. The filtering of the raw data was carried out using 4 functions that eliminate LiDAR returns from areas of non-interest associated with: (1) the ground in the inter-row, (2) adjacent rows, (3) undervine and inter-row vegetation (weeds) and (4) obstacles too close to the sensor to be canopy.

(1) Inter-row ground filtering: beams intercepted by the ground in the inter-row must be removed from the raw data. It is assumed that this zone corresponds to half of the distance from the sensor to the line of trunks and equates to a distance D_δ of 0.625 m in these vineyards (Figure 2). Depending on the height of the LiDAR (HS), the beams in the interval $[0; \delta]$ are removed. D_δ is not fixed and should be adjusted for changes in row width and canopy vigour and shape if transferred to other production systems. The value of the angle δ is calculated as follows:

$$\delta = atan\left(\frac{D_\delta}{HS}\right)$$

(2) Filtering of adjacent rows: in a first pass, points intercepted more than two rows away (> 8 m) from the LiDAR sensor were removed from the raw data. Then, assuming that the tractor has a straight trajectory centred in the inter-row, with a systematic error of ± 0.035 m, the distance from the centre of the inter-row to the trunk line (LoT) can be used to identify and delete points associated with the opposite side of the canopy or adjacent rows. The filter value (D) is therefore half the row width (D_{ir}).

$$D = \left(\frac{D_{ir}}{2}\right)$$

(3) Grassed zone filtering: vegetation present under the vine or in the inter-row must be removed from the raw data to avoid its inclusion in the calculation of the vegetative parameters. For this purpose, the height of the grassed zone (HG) could be set as a constant threshold, which would need to be adjusted between systems, or alternatively derived from the LiDAR data, so that it is automated. In the latter case, HG can be derived under the assumption that there is only grass below the LiDAR sensor and that HS is known. In this case, a distance for filtering the grassed zone (D_{ε}) can be defined as:

$$D_{\varepsilon} = D - D_{\delta}$$

The beams are removed at the angles ε in the interval that is considered as the grassed zone (Figure 2). The value of the ε angle is defined as:

$$\varepsilon = atan\left(\frac{D_{\varepsilon}}{HS}\right)$$

Subsequently, a distance H_{ε} can be calculated as the average distance of the nearest 5% of intercepted points to the LiDAR emission point in the grassed zone, as defined by the angle ε. The 5% threshold was based on previous unpublished research using this setup. HG is therefore defined as:

$$HG = HS - H_{\varepsilon}$$

This filtration threshold (HG) will evolve during the season according to the acquisition date and the characteristics of the ground cover in the blocks (Figure 2). The angle ε may need to be altered in vineyards with differing canopy and ground cover conditions to those in southern France. The relative importance of this filter will vary depending on how precisely ground cover in the vineyard is managed.

(4) Near point filtering: beams intercepted at a distance too close to the 2D LiDAR to be canopy need to be removed from the raw data. Most of these are likely to be associated with large insects or random, untrained or broken shoots. The filter value was set at a constant 0.5 m, which was based on the operating range of the 2D LiDAR sensor and the expectation that the canopy is vertically trained (Figure 2). This fixed threshold will again need to be adapted when transferred into vineyards with different training and trellising modes; however, once determined, it should be a fixed value to automate this filtering process. In practice, this filtering represents a tiny fraction of point removal by AFM.

Before the application of these four filters, no pre-processing or filtering was applied to the raw point clouds. Generic parameters based on vineyard characteristics were set and all the above defined filters were applied automatically. At the end of this step, it was possible to separate the intercepted points into two categories (Figure 2): (1) points intercepted outside the zone of interest (in blue) that have

been eliminated, and (2) points intercepted in the zone of interest (trunk, vegetation and trellis wire) (in red).

Figure 2 near here

2.4.2.2. Clustering methodology

The determination of canopy dimensions from the pre-processed LiDAR data consisted of two parts; (a) a 1D cluster analysis based on the vegetation height from the LiDAR point clouds to identify different components of the vine and trellis, followed by a Bayes classification, and (b) a statistical test (thresholding) to delimit two dimensional parameters (vegetation height and vegetation width), associated with the canopy area defined from the classification process.

(a) 1D hierarchical cluster and Bayes classification

The LiDAR point cloud expressed the canopy information in a 3D space. Points therefore corresponded to heterogeneous distributions, like multivariate clusters, of discrete objects within the sample space according to their positioning. Field observations suggested the presence of at least three different 'groups' within the general area of interest for the canopy. A "low" group associated with LiDAR returns from the trunk and low-hanging or poorly placed shoots; a "high" group, particularly early in the season, associated with LiDAR returns from trellis wires and infrastructure; and a "transition" or central group associated with LiDAR returns from the canopy (Figures. 3A, 3B and 3C). The spatial location (on a vertical axis) of the high and low groups is static, as the trellis wires and vine trunks are fixed. It is predominantly the transition group associated with the canopy that is dynamic and changing as the season progresses. As the vine grows, the transition group will merge with the high group and obstruct the trellising wires.

Hierarchical cluster analysis was performed to determine if there were two or three unique combinations of Gaussian distributions along the height axis. Given the expected overlapping Gaussian distributions of the 2D LiDAR groups, a hierarchical clustering algorithm based on a Gaussian mixing model (Fraley et al., 2007) was used. Hierarchical clustering defines classes by grouping the most similar observations in a hierarchical fashion and is based on functions that combine model-based hierarchical clustering (expectation–maximisation) and the Bayesian Information Criterion (BIC). The clustering was conducted using the mclust package (Fraley et al., 2012) in R.

Once the points in the point cloud had been clustered and points associated with (or likely to be associated with) the canopy had been identified, the canopy dimensions were calculated. The canopy point cloud will follow a Gaussian distribution (Figures. 3A, 3B and 3C). Therefore, a choice must be made on which values of this distribution should be used to determine canopy dimensions. In the standard approach of Rinaldi et al. (2013), extreme values were used for width and for the maximum height, while the minimum height (Hsc) was defined manually as the cordon height. However, in the case of an automated system, as proposed here, this may not be sensible as some outlying values may be retained and will unduly influence the dimension calculations. A sensitivity analysis on the choice of a statistical threshold for defining the vegetation height and width was carried out. The distribution of the points along the y axis were filtered based on standard deviations (σ_H) from the population mean (μ_H). The thresholds were established as follows: μ_H +/- (β_H * σ_H) with β_H a parameter. Candidate values for β_H were selected as follows: 0.5; 1; 1.5; 2; 2.5; 3. For each set of data corresponding to the same phenological stage (from T1 to T7) and for each β_H values (6 in total), the absolute error

(expressed in m) between the dimensions of the vegetation canopy measured manually by an operator in the field and estimated by the clustering method was calculated for the vegetation. Any y-values that were not in the respective interval were excluded from the analysis. The evolution of the absolute error according to the selected candidate β_H values allowed the identification of the optimum β_H value that minimised the absolute error (vs. manual measurement). Thus, a set of seven phenology dependent β_H thresholds were defined that covered the whole season.

With regards to the estimation of canopy width, a similar sensitivity analysis was carried out in the z axis using the methodology described above for canopy height (y axis). However, as only one side of the vine was scanned, a symmetry hypothesis was used based on the observations of Arnó et al. (2015) to estimate full canopy width from half canopy width. The half width of canopy was estimated using the line of trunks (LoT) as the upper limit. The z-values of the point cloud followed an exponential distribution over the interval [μ_w - (β_w * σ_w); LoT]. The lower thresholds were established as follows: μ_w - (β_w * σ_w) (with μ_w and σ_w respectively the mean and standard deviation of the z values of the points defined in the foliar zone). For each phenological stage and for each β_w value, the absolute error was calculated (expressed in m) between the manually measured full canopy width and the canopy width estimated by the clustering method. Calculating this over a range values (0.5; 1; 1.5; 2; 2.5; 3) allowed an adjustable threshold (β_w) to be defined at each observed phenological stage along the season that minimised the absolute error against the manual measurements.

The parameterisation of the adjustable (temporal) threshold for defining the canopy zone was carried out for different phenological stages. This is needed because (1) the number of groups defined by the algorithm changes with vine development, decreasing from three at the start of the season to two groups by mid/late-season once the trellising wire is covered by foliage and (2) the geometry of the canopy evolves with vine management operations, such as lifting, trimming and topping, that are linked to phenological development, and they have a potential impact on canopy dimensions.

(b) Estimation of canopy height and width based on adaptive thresholding in the canopy zone

Given the preferred β_H and β_w values for the vine phenological stage, canopy dimensions in the y and z axes can be derived from the 2D LiDAR points classed as the canopy zone. Height and width were calculated for each vine unit.

Vegetation height (VH) in m was defined as:

$$VH = (\mu_H + (\beta_H * \sigma_H)) - (\mu_H - (\beta_H * \sigma_H))$$

where β_H is the threshold identified from the sensitivity analysis for a particular phenological stage; μ_H and σ_H are respectively the mean and standard deviation of the y values defined in the canopy zone

Vegetation width (VW) in metre (m) was derived from a LiDAR scan of only one side of the vineyard row. Therefore, VW was calculated as double the width of one side and defined as:

$$VW = (D - (\mu_w - (\beta_w * \sigma_w)) * 2$$

where D is the distance between the LiDAR travel line and the LoT (in m), βw is the threshold identified from the sensitivity analysis for a particular phenological stage and μ_w and σ_w are respectively the mean and standard deviation of the z values defined in the canopy zone.

2.5. Error assessment of result

2.5.1. Quantitative comparison of filter methods

In order to compare the effect of the AFM (first step in the BPCC) and the PROTOLIDAR package on the raw point cloud data, both approaches were compared with an intensive expert classification of the entire point cloud, which is termed a "Human Expert Filtration" (HEF) approach. The HEF consisted of manually tagging all the intercepted points and using the expert's knowledge to classify each LiDAR return into a group (inter-row ground, adjacent rows, grassed zone, near point or canopy). This was a very laborious process and was only performed on a few vine units at different phenological stages to illustrate and compare how the three different filtering methods were performing. To describe the differences between the HEF, the PROTOLIDAR and AFM methodologies, a distribution of the intercepted points in the four groups defined by the applied filters was studied and a comparison of the percentage of the points retained to calculate vegetative parameters after the filtration steps was performed on two 3D LiDAR point clouds from an acquisition made on three vines (*Vitis vinifera* L. cv. Marselan) at three different stages - BBCH 14, 57 and 76 (Table 1). It should be noted that the PROTOLIDAR method is a global and non-specific method for filtering intercepted LiDAR points. It did not offer the possibility to class the filtered points according to groups (inter-row ground, grassed zone, etc). Consequently, only total data removed, and not associated groupings, are reported for the PROTOLIDAR method.

2.5.2. Sensitivity study on thresholding in the clustering methodology

A sensitivity analysis was used to select β_H and β_w thresholds that minimised the absolute difference with manual measurement of canopy dimensions. To evaluate the accuracy and precision of the automatic clustering method within the sensitivity analysis, several statistical tests were performed on the absolute errors measured on the 560 vine units. To test the accuracy between the different methods, an ANOVA test was performed on the absolute error values per vine unit by aggregating the data for each phenological stage (n = 80 vine units) and significant differences between the groups determined by a Tukey Honest Significance Difference (Tukey-HSD) post-hoc test. The variance of the absolute error is a measure of the precision of the method, with a low variance indicating a high precision. To test for differences in the variance between groups, a pairwise test was done using Bartlett's test ($\alpha = 0.05$) and p values were adjusted using the Bonferroni method (Westfall et al., 1997).

2.5.3. Comparison of derived canopy dimensions between the PROTOLIDAR - BPCC - CMM methodologies

The coefficient of variation of root mean square error (CV-RMSE) and the correlation coefficient of concordance (CCC; Lin et al. 1989) were calculated to evaluate the quality and concordance of the estimations of canopy height and width between the established methods (PROTOLIDAR and manual observations) and the new method (BPCC) for all vine units over the entire season. The R^2 was used to evaluate the fit of these regressions.

3. Results and discussions

3.1. Quantitative comparison of filtering methods

Table 1 shows the number of points removed and the percentage of points retained using the three different filtration methods for three vine units in one vineyard (*Vitis vinifera* L. cv. Marselan), representing three of the phenological stages measured (14, 57 and 76). The results in Table 1 are presented to illustrate the behaviour of the three filters, not to present a complete analysis over all 560 vines. The HEF approach is slow and laborious and could not be performed on all vines. It can be observed that the total number of points intercepted increased throughout the growing season, as the canopy size increased. The percentage of points retained differed between the PROTOLIDAR and

AFM (Table 1), with more points preserved with the AFM regardless of the phenological stage. There were respectively 2%, 9% and 12% more points preserved with the AFM at BBCH 14, 57 and 76. Although the HEF method retained the highest percentage of points for all three phenological stages, it retained on average only 1.3 % more points than the AFM. Overall the removal rate was approximately 50 - 60% of the data for the three filters and three stages (Table 1). This is expected considering the wide scan angle relative to the canopy area that results in a large amount of data being collected from areas of non-interest. The similarity between HEF and AFM in these three vine units indicated that AFM retained a sensible level of information for subsequent analysis. Overall, the AFM method mimicked the expert approach more closely and retained a larger percentage of data to carry through to the next stage than the PROTOLIDAR method.

At BBCH 14, there was little difference between the AFM and PROTOLIDAR methodologies (Table 1). This can be explained by the almost non-existent grassed zone that limited errors when classifying the canopy zone. Additionally, at this growth stage, vegetation was sparse permitting the LiDAR laser beams to penetrate the inner surface of the canopy. There was no shadowing effect, allowing the PROTOLIDAR method to estimate the canopy area with high precision. However, at more advanced growth stages (BBCH 57 and 76) there was a significant difference between the AFM and PROTOLIDAR filtration methods with the PROTOLIDAR filter removing more points.

The PROTOLIDAR methodology only relies on this filtering step to eliminate erroneous data and to define the canopy zone. Thus, the accuracy of the filtering directly affects the accuracy of the PROTOLIDAR estimations of canopy dimensions. In addition, it should be noted that the PROTOLIDAR method is based on a hypothesis of total propagation of LiDAR laser beams through the vegetation to define the canopy width. However, with high-density canopies, the LiDAR beams cannot penetrate deeply in or through the canopy. Instead the majority of the LiDAR returns are from the outer surface of the canopy. This is a "shadowing effect" and reduces the amount of information related to the inner surface of the canopy. Returns from the far-side of dense canopies are very limited, reducing the precision of canopy width estimations. This shadowing effect is one of the main drawbacks of the laser measurement system (Van der Zande et al., 2006).

While Table 1 provides an example comparison including the HEF approach, the filtered points from AFM and PROTOLIDAR methods were calculated and compared over the entire vegetation season from the 560 vine units. From this global analysis, the AFM method retained on average 9% more points than the PROTOLIDAR method for calculating canopy dimensions (data not shown). However, it should be noted that the performance of PROTOLIDAR filtering may be affected by imperfect adjustment of filtering parameters. Although a considerable amount of time was spent manually optimising the filter parameter settings, there may be a better set of parameters that could have been used for the 560 vine units used for comparison.

Table 1. Points deleted from three different filtration methods, for three vine units in one vineyard (*Vitis vinifera* L. cv. Marselan) at BBCH stages 14, 57 and 76 to illustrate the differences between the automatic filtration method (AFM), the human expert filtration (HEF) and the PROTOLIDAR methodologies. Deleted points are classed according to the four groups defined in the AFM. The percentage of points retained by each filter at each stage indicates the data that are available to be used in the derivation of canopy dimensions post-filtration.

Methodology	Number of deleted points after filtration step				Percentage of points retained after filtration step
	Inter-row ground	Grassed zone	Adjacent rows	Near points	
BBCH 14 - total number of intercepted points in the vine unit = 2732					
HEF	450	154	966	0	43
PROTOLIDAR	NA†	NA†	NA†	NA†	39
AFM	470	149	986	0	41
BBCH 57 - total number of intercepted points in the vine unit = 4136					
HEF	469	387	1244	34	48
PROTOLIDAR	NA†	NA†	NA†	NA†	37
AFM	479	377	1335	34	46
BBCH 76 - total number of intercepted points in the vine unit = 5014					
HEF	542	489	1345	0	52
PROTOLIDAR	NA†	NA†	NA†	NA†	39
AFM	562	501	1369	0	51

† The PROTOLIDAR filter did not permit classification of deleted points into groups

3.2. Sensitivity study on thresholding in the clustering methodology

This analysis concerned the influence of the statistical thresholds, β_H and β_w, on the calculation of vegetation height (VH) and width (VW) in the clustering method. The evolution of the absolute errors (in m) between canopy height and width from CMM and VH and VW are shown in Tables 2 and 3 respectively. For both VH and VW, the values of β_H and β_w that minimised the absolute error when compared with CMM were not constant during the growing season. Table 2 shows that for the phenological stages BBCH 14, 53 and 57, a value of 2 for β_H (equivalent to ±2 σ or the retention of 95 % of the data) gave the lowest absolute error to define the canopy height from the BPCC filtered LiDAR data. However, for phenological stages BBCH 61 and 81, a value of 3 (±3 σ or retention of 99.7 % of the data) minimised the absolute error relative to CMM. This is explained by the elongation and the lifting of shoots between BBCH 57 and 61 that moves the canopy into and above the upper trellis wire. Before this, there is a clear third (high) group associated with LiDAR returns from the upper trellis wire that needs to be considered in the determination of canopy dimensions.

The sensitivity analysis associated with β_w indicated a preferred value of 2 for the earliest and latest observed phenological stages (BBCH 14 and 81), and a value of 3 for all other stages in order to reduce the absolute error. Thus a more severe trimming (lower β_w value) is needed early and late in the season. No clear reason was found for this empirical result. It may be associated with a less dense canopy (more open foliage) at both these phenological stages that is associated respectively with early-season leaf/shoot expansion and late-season leaf senescence.

The best performed thresholds (β_H and β_w) at each phenological stage are shown in bold in Tables 2 and 3. The absolute errors between canopy height and width from the PROTOLIDAR and CMM at

554 each phenological stage are also shown. This permits an indirect comparison of absolute error for the
555 BPCC and PROTOLIDAR methods (both relative to CMM). For canopy height, the optimised BPCC
556 method outperformed (lower absolute error) the PROTOLIDAR at all phenological stages, with the
557 difference in absolute error rising from 0.08 m early in the season to 0.16 m late in the season (Table
558 2). For canopy width, the response was different. Earlier in the season (BBCH 14), when the
559 vegetation was not very dense, the absolute error associated with the PROTOLIDAR method was less
560 than the BPCC method (0.11 m vs 0.17 m respectively) (Table 3). However, as the canopy developed
561 and the vegetation became denser, the optimised BPCC estimated canopy width with less absolute
562 error than PROTOLIDAR, with an average difference ≥ 0.16 m from BBCH 61 onwards (Table 3).
563 This can be explained by the increasing influence of shadowing effects in the LiDAR data as the
564 canopy develops. The PROTOLIDAR depends on LiDAR returns from the distal part of the canopy to
565 estimate canopy width. With larger, denser canopies, these returns are greatly reduced, generating less
566 certainty in the shape of the distal part of the canopy and therefore more error in canopy width
567 estimation. Under these conditions, it appears that an estimation of canopy width based on half-row
568 LiDAR scans and the assumption of a symmetrical canopy structure is more accurate. The
569 PROTOLIDAR method was developed under the assumption that a good quality 3D point cloud of the
570 canopy is available, i.e. scanned from both sides in the case of larger canopies. It is not surprising that
571 the absolute error with the PROTOLIDAR canopy width estimations increases overtime with canopy
572 development. However, as noted in the introduction, a clear need for the industry is to have LiDAR
573 processing systems that can operate with half-row scans. The BPCC method permitted estimations of
574 the height and width of individual vine canopies (i.e. a site-specific estimation) with absolute errors <
575 0.2 m in both height and width at any point throughout the season and < 0.15 m at growth stages up to
576 and including flowering (BBCH 61). The exception to this was canopy width estimations very early in
577 the season (BBCHH 14) with BPCC (absolute error compared to CMM was 0.17 m). However, at this
578 stage, the canopy is still small, shoots can still be randomly organised thereby generating measurement
579 or scanning anomalies, and issues with PPP coverage are unlikely in small open canopies. Therefore,
580 this result was not considered detrimental to the potential adoption of the BPCC.
581
582 The sensitivity analysis of both β_H and β_w indicated that a dynamic threshold value is preferable for
583 calculating vegetation height and width with the clustering method. The optimum threshold can be
584 associated with the management and the architecture of the vine, that itself can be modelled or sensed,
585 enabling the threshold to be programmed in the clustering method based on vine management and
586 phenology. This makes the BPCC less subject than PROTOLIDAR to operator interpretation for
587 calculating VW, particularly at the beginning and end of the season (Table 3). It should be noted that
588 the absolute error was highest towards the end of the season, a period when, typically, PPP are applied
589 less frequently in vineyards. In this study, the parameterisation of the number of clusters defined by
590 the algorithm was performed in a supervised mode. In future developments, a statistical test could be
591 used to support the automatic determination of the number of clusters to be defined. This would be
592 important in vineyards at mid-season when there is potentially a clear difference between high and low
593 vigour areas in a vineyard in regards to the location of shoots relative to the upper trellis wire.
594

595 Table 2. Pairwise differences of the means of absolute errors (in m) for the vegetation height
596 parameter of the conventional manual measurement (CMM) and PROTOLIDAR and clustering
597 methodologies, grouped by BBCH stage class with *p* value from ANOVA. Variances between groups
598 that differed significantly using Bartlett's test with the Bonferroni adjustment are in italics.
599 Considering the clustering method, for each BBCH stage, the β_H threshold that minimised the absolute
600 mean error rate with CMM is in bold.
601

Stage BBCH	*clustering* β_H *=1*	*clustering* β_H *=2*	*clustering* β_H *=3*	*PROTOLIDAR*	*p-value*
14	0.14	**0.08**	*0.21*	0.12	$p <$ 0.001
53	0.14	**0.09**	0.24	0.14	$p <$ 0.001
57	0.18	**0.11**	0.33	0.17	$p =$ 0.017
61	0.24	0.21	**0.12**	0.19	$p =$ 0.038
70	*0.25*	0.23	**0.13**	0.21	$p =$ 0.027
76	0.33	0.29	**0.14**	0.24	$p =$ 0.039
81	0.36	0.32	**0.16**	0.26	$p =$ 0.025

602
603 Table 3. Pairwise differences of the means of absolute errors (in m) for the vegetation width parameter
604 of the conventional manual measurement (CMM) and PROTOLIDAR and clustering methodologies,
605 grouped by BBCH stage and with *p* value from ANOVA. Variances between groups that differed
606 significantly using Bartlett's test with the Bonferroni adjustment are in italics. Considering the
607 clustering method, for each BBCH stage, the β_w threshold that minimised the absolute mean error rate
608 with CMM is in bold.

Stage BBCH	*clustering* β_w *=1*	*clustering* β_w *=2*	*clustering* β_w *=3*	*PROTOLIDAR*	*p-value*
14	*0.37*	0.28	**0.17**	0.11	$p = 0.019$
53	0.38	**0.11**	0.21	0.18	$p = 0.027$
57	0.22	**0.13**	0.26	0.21	$p = 0.032$
61	*0.36*	**0.14**	0.22	0.24	$p = 0.041$
70	0.20	**0.17**	0.29	0.28	$p = 0.038$
76	*0.32*	**0.19**	0.24	0.31	$p = 0.026$
81	0.39	0.28	**0.19**	0.32	$p = 0.039$

609
610 ***3.3. Classification of the intercepted points of a 3D LiDAR point cloud***
611 In order to illustrate the classification method used by the BPCC, a detailed analysis was performed on
612 a single vine unit at three phenological stages for height (Figures 3 and 4) and width (Figure 5). Figure
613 3 presents histograms of the points intercepted in the different compartments of a vine (trunk, leaf area
614 and trellis wires) along the height axis (y) at BBCH 14, 57 and 76. It visualises the change in the
615 number of defined clusters during the season, with a decrease from three to two clusters after BBCH
616 61, when the upper trellis wire is covered by the canopy (Figure 3C). The adaptive threshold for the
617 grassed zone filter (HG) also changed during the season, increasing from 0.25 m at BBCH 14 (Figure
618 3A) to 0.35 m at BBCH 76 (Figure 3C). Across all 560 vines, HG varied between 0 and 0.4 m on
619 different days and in different blocks (data not shown). The distribution of intercepted points in the
620 canopy zone followed a Gaussian distribution throughout the growing season (solid black lines in

Figure 3). Independently of phenological stage, a higher number of intercepted points, associated with a higher density of vegetation, was found in the centre of the canopy zone (in green) (Figures 3A-C). This can be explained by the Royat cordon training system used in this block. This is explained by the presence of primary shoots and the first three leaves in the central zone at the beginning of vegetation (BBCH 14), by the appearance of flower buds which are transformed into bunches mid-season (BBCH 57), and by the mechanical action of pruning, which induces the development of secondary shoots in the central zone of the canopy later in the season (BBCH 76).

Figure 4 presents similar information to the statistical distributions in Figure 3, but in the form of a 2D plot along the row. It clearly illustrates changes in LiDAR returns associated with the under-vine grassed zone as well as canopy height over the course of the season. The issue with the proximity of the upper canopy to the upper trellis wire mid-season (Figure 4B) and its potential effect on the PROTOLIDAR method for height estimation is clear. While the PROTOLIDAR overestimated height at BBCH 57 (and similar stages), the use of a three-class hierarchical clustering with a moderate level of trimming ($\beta_H = 2$) provided more accurate canopy height (VH) estimations (Table 2).

Figure 3 near here

Figure 4 near here

An alternative view of the LiDAR returns from the same vine, at the same three phenological stages, to illustrate changes in canopy width is shown in Figure 5. This is a cross-section through the canopy of a scan taken from the left-hand side of the image. Early in the season, the small vine size allows a good characterisation of the full canopy from the half-row scan (Figure 5A). However, as noted previously, the characterisation of the distal side of the canopy is problematic with half-row scans as the canopy develops, which leads to issues with underestimating full canopy width with the PROTOLIDAR method. The decrease in the density of LiDAR returns from the far side of the canopy is obvious from midseason onwards (Figures 5B-C).

Figure 5 near here

3.4. Comparison of canopy dimensions derived from the PROTOLIDAR - BPCC - CMM methodologies

Table 4 presents the CCC, R^2 and CV-RMSE statistics from comparisons of estimations of canopy height and width from the BPCC, PROTOLIDAR and CMM on all 560 vine units. The CMM was considered as a reference observation. There was a strong statistical relationship between all pairwise comparisons (Table 4). The BPCC generated similar results to the PROTOLIDAR, with height estimations slightly more similar than width estimations between the two methods. This indicated that the proposed automated approach was similar to the more manually demanding PROTOLIDAR method for vegetation height and width estimation. It is acknowledged that the relationship between the width estimations is likely to change if the PROTOLIDAR method is applied to a full canopy scan as it was initially intended to be.

When compared with CMM, the BPCC slightly outperformed PROTOLIDAR (higher CCC and R^2 and lower CV-RMSE) for the estimation of canopy height and width. However, for both approaches the relationship with CMM was strong over the entire season. For height, the improved fit with BPCC resulted from the two stage filtering and classification approach that adapted to canopy development and provided more accurate mid- and late-season estimations. For width, the PROTOLIDAR was more accurate at early stages, when the canopy was small and open, allowing impacts to be made

throughout the canopy (Table 3). As canopy size and density increased, impacts were less likely to occur in distal parts of the canopy and width estimations with the PROTOLIDAR from a half-row scan became less accurate than the BPCC method, which assumed symmetry and a fixed distance from the LoT (Table 3).

Table 4. Results of the comparison between PROTOLIDAR methodology, a LiDAR Bayesian point cloud classification algorithm (BPCC) and conventional manual measurement (CMM) in the estimation of vegetation height (VH) and width (VW) for all vines over the entire season.

Pairwise comparisons		CCC		R^2		CV-RMSE (%)	
		VH	VW	VH	VW	VH	VW
PROTOLIDAR	*BPCC*	0.97	0.92	0.94	0.89	5	7
PROTOLIDAR	*CMM*	0.92	0.87	0.91	0.83	12	15
BPCC	*CMM*	0.94	0.90	0.92	0.85	10	13

3.5. Future applications for dose management of PPP and precision viticulture

The method for expressing PPP doses currently used in French viticulture is based on a fixed dose, defined per ha ground surface area (Codis et al., 2016). In this context, a system for expressing PPP doses that explicitly takes into account the evolution of the structure of the plant to be protected, as well as spatial variability in this evolution, would be an important step toward more efficient agricultural practices. The development of precision spraying technologies has been identified as a key area for more efficient viticulture (and agriculture) practices (Berk et al., 2016). As such, the automated method for analysis of LiDAR point clouds proposed here is an important step forward. In this work, the method and validation were focussed on the determination of canopy dimensions from sensor data. By themselves, canopy dimensions are limited. Once obtained they are typically used to calculate vegetative indicators, such as the TRV indicator that has been used to adjust PPP dose rates in Switzerland (Viret and Höhn, 2008). More recently, the LWA indicator has been proposed by the chemical industry as a new method to report dose expression at the European level (Wohlhauser, 2009). Ideally these indicators, which have both been used for dose adjustment and dose expression (Llorens et al., 2010; Walklate et al., 2011), should also incorporate information related to canopy density/porosity for still more accurate dose management (Pergher and Petris, 2008).

However, when these vegetative indicators are manually determined, there is still a possibility that the canopy structure metric is over- or under-estimated (Rüegg et al., 2001). Predictive modelling and real-time observation of spray deposition patterns are capable of providing a feed-back mechanism to correct misapplications (either over or under applications) (Saddem et al., 2017). These are not yet well developed or commercialised but they could also form an important part of any future PPP application system.

Vineyards and orchards present a wide variety of different canopy characteristics. Although the results presented here are only from one vineyard (over four different blocks) scenario, the BPCC has been designed to be flexible so that it can be adapted to a variety of training systems and production situations. The choice of thresholds used here may need to be altered for other types of production systems, and the relative importance of the four filtering algorithms in the AFM may change. However, once the parameters and thresholds have been set, the algorithm should run in a fully automated manner, permitting it to be used in on-the-go applications.

The concept of Line of Trunks (LoT) (del-Moral-Martínez et al. 2015) and the use of vine symmetry (Arnó et al., 2015) to model canopy width have been used here. This permitted a more automated approach to modelling canopy width and generated better estimates of canopy width from one-sided canopy scans from BBCH 53 (mid- and late-season) (Table 3). Early season width estimations were better with PROTOLIDAR but the mean absolute error at BBCH 14 was low for BPCC (0.17 m). The accuracy achieved with BPCC negated the need for scanning both sides of the canopy. This is important as scanning both sides requires the fusion of point clouds from both sides, with issues such as rectification and harmonisation. Considering multi-row spraying, scanning only one canopy side means fewer LiDAR sensing systems to be installed on a sprayer with real-time dose control.

Although focussed on canopy dimensions here, the automatic classification of different components of vines potentially provides additional, automatically collected information that could be used for vine and vineyard management, e.g. spraying for variable grass height/growth or estimating vine trunk diameter.

4. Conclusions

In this study, a LiDAR BPCC was proposed that combined an AFM and a clustering method to automate the 3D digital characterisation of the dimensions of vineyard canopies from LiDAR data. The BPCC only required basic configuration related to vineyard set up to operate autonomously. To evaluate the efficacy of the BPCC filtering of LiDAR point clouds, it was compared to a manual human expert filter (HEF) and to a semi-automatic method requiring manual pre-processing (PROTOLIDAR). The results obtained from data collected on several grape varieties in a two different training modes demonstrated that the BPCC filtered the LiDAR point clouds in an equivalent way to HEF and to the well-accepted PROTOLIDAR research method. Hierarchical classification and trimming of the AFM filtered LiDAR data yielded estimations of canopy height and width that were strongly correlated with equivalent PROTOLIDAR estimations. The classification was most effective when the threshold in the trimming process was permitted to be variable along the season. Empirical results provided clear indications of the preferred threshold value for both height and width at different phenological stages. When a dynamic threshold was used, the canopy dimensions from the BPCC process were closer to manual canopy observations than the equivalent PROTOLIDAR estimations. These results demonstrated that although operating at a higher level of automation, which is more suited to on-the-go processing, the proposed BPCC was more effective than the PROTOLIDAR to filter point cloud data and to estimate canopy dimensions in vineyards from half-row scans. This is a first iteration of a potential automated LiDAR processing algorithm. Further improvements are needed before commercial deployment, in particular to provide a more robust temporal estimator for the determination of the trimming threshold and for determining the preferred number of classes for a given phenological stage or canopy size. The BPCC method also needs to be validated over other training systems.

Acknowledgments

The authors are indebted to the numerous individuals that assisted in collecting the field data presented in this work: Hudebine Y., Riberolles X., Trinquier E., Delpuech X., Rico A., de Jesus P., Delpuech X., Verges A., Lienard A., Kazakos A., Mariette A., de Runicki V., Bastianelli M. We also want to thank the staff members of the vine estate Domaine Mas Piquet for making their plots available for our measurements. The first author also addresses his personal thanks to especially Abdelghani Cheraiet and Louisa Moussaoui.

This work was supported by the French National Research Agency under the Investments for the Future Program, referred to as ANR-16-CONV-0004. Anice Cheraiet's PhD is cofunded by #DigitAg and IFV Acta.

References

Andersen, H. J., Reng, L., & Kirk, K. (2005). Geometric plant properties by relaxed stereo vision using simulated annealing. Computers and Electronics in Agriculture, 49(2), 219-232. https://doi.org/10.1016/j.compag.2005.02.015

Arnó, J., Escolà, A., Vallès, J. M., Llorens, J., Sanz, R., Masip, J., Palacín, J., & Rosell-Polo, J. R. (2013). Leaf area index estimation in vineyards using a ground-based LiDAR scanner. Precision Agriculture, 14(3), 290-306. https://doi.org/10.1007/s11119-012-9295-0

Arnó, J., Escolà, A., Masip, J., & Rosell-Polo, J. R. (2015). Influence of the scanned side of the row in terrestrial laser sensor applications in vineyards: Practical consequences. Precision Agriculture, 16(2), 119-128. https://doi.org/10.1007/s11119-014-9364-7

Arnó, J., Escolà, A., & Rosell-Polo, J. R. (2017). Setting the optimal length to be scanned in rows of vines by using mobile terrestrial laser scanners. Precision Agriculture, 18(2), 145-151. https://doi.org/10.1007/s11119-016-9451-z

Bastianelli, M., Rudnicki, V. D., Codis, S., Ribeyrolles, X., & Naud, O. (2017). Two vegetation indicators from 2D ground Lidar scanner compared for predicting spraying deposits on grapevine. Proceedings of the 2017 EFITA WCCA conference, Montpellier, France, 153-154.

Berk, P., Hocevar, M., Stajnko, D., & Belsak, A. (2016). Development of alternative plant protection product application techniques in orchards, based on measurement sensing systems: A review. Computers and Electronics in Agriculture, 124, 273-288. https://doi.org/10.1016/j.compag.2016.04.018

Byers, R. E., Hickey, K. D., & Hill, C. H. (1971). Base gallonage per acre. Virginia Fruit, 60(8), 19-23.

Campos, J., Llop, J., Gallart, M., García-Ruiz, F., Gras, A., Salcedo, R., & Gil, E. (2019). Development of canopy vigour maps using UAV for site-specific management during vineyard spraying process. Precision Agriculture, 20(6), 1136-1156. https://doi.org/10.1007/s11119-019-09643-z

Codis, S. (2016). Stakes for a new model of dose expression in viticulture: advantages and points to be taken into consideration. In Proceedings of the EPPO Workshop on harmonized dose expression for the zonal evaluation of plant protection products in high growing crops, Austrian Agency for Health and Food Safety Vienna,12-13.

Colaço, A. F., Molin, J. P., Rosell-Polo, J. R., & Escolà, A. (2018). Application of light detection and ranging and ultrasonic sensors to high-throughput phenotyping and precision horticulture: Current status and challenges. Horticulture research, 5(1), 1-11. https://doi.org/10.1038/s41438-018-0043-0

de Castro, A., Jiménez-Brenes, F., Torres-Sánchez, J., Peña, J., Borra-Serrano, I., & López-Granados, F. (2018). 3-D Characterization of Vineyards Using a Novel UAV Imagery-Based OBIA Procedure for Precision Viticulture Applications. Remote Sensing, 10(4), 584. https://doi.org/10.3390/rs10040584

del-Moral-Martínez, I., Arnó, J., Escolà, A., Sanz, R., Masip-Vilalta, J., Company-Messa, J., & Rosell-Polo, J. (2015). Georeferenced Scanning System to Estimate the Leaf Wall Area in Tree Crops. Sensors, 15(4), 8382-8405. https://doi.org/10.3390/s150408382

del-Moral-Martinez, I., Rosell-Polo, J. R., Company, J., Sanz, R., Masip, J., Martínez-Casasnovas, J. A., & Arnó, J. (2016). Mapping Vineyard Leaf Area Using Mobile Terrestrial Laser Scanners: Should Rows be Scanned On-the-Go or Discontinuously Sampled? Sensors, 16(1), 119. https://doi.org/10.3390/s16010119

Escolà, A., Martínez-Casasnovas, J. A., Rufat, J., Arnó, J., Arbonés, A., Sebé, F., Pascual, M., Gregorio, E., Rosell-Polo, J. R. (2017). Mobile terrestrial laser scanner applications in precision

fruticulture/horticulture and tools to extract information from canopy point clouds. Precision Agriculture, 18(1), 111–132. https://doi.org/10.1007/s11119-016-9474-5
Fraley, C., & Raftery, A. (2007). Model-based Methods of Classification : Using the mclust Software in Chemometrics. Journal of Statistical Software, 18(6). https://doi.org/10.18637/jss.v018.i06
Fraley, C., & Raftery, A. E. (2012). Mclust Version 4 for R: Normal Mixture Modeling for Model-Based Clustering, Classification, and Density Estimation. Technical Report No. 597. Department of Statistics, University of Washington.
Gil, E., Escolà, A., Rosell, J. R., Planas, S., & Val, L. (2007). Variable rate application of plant protection products in vineyard using ultrasonic sensors. Crop Protection, 26(8), 1287-1297. https://doi.org/10.1016/j.cropro.2006.11.003
Gil, E., Llorens, J., Llop, J., Fàbregas, X., Escolà, A., & Rosell-Polo, J. R. (2013). Variable rate sprayer. Part 2 – Vineyard prototype: Design, implementation, and validation. Computers and Electronics in Agriculture, 95, 136-150. https://doi.org/10.1016/j.compag.2013.02.010
Gil, E., Arnó, J., Llorens, J., Sanz, R., Llop, J., Rosell-Polo, J., Gallart, M., & Escolà, A. (2014). Advanced Technologies for the Improvement of Spray Application Techniques in Spanish Viticulture: An Overview. Sensors, 14(1), 691-708. https://doi.org/10.3390/s140100691
Jaakkola, A., Hyyppä, J., Kukko, A., Yu, X., Kaartinen, H., Lehtomäki, M., & Lin, Y. (2010). A low-cost multi-sensoral mobile mapping system and its feasibility for tree measurements. ISPRS Journal of Photogrammetry and Remote Sensing, 65(6), 514-522. https://doi.org/10.1016/j.isprsjprs.2010.08.002
Lee, K. H., & Ehsani, R. (2009). A Laser Scanner Based Measurement System for Quantification of Citrus Tree Geometric Characteristics. Applied Engineering in Agriculture, 25(5), 777-788. https://doi.org/10.13031/2013.28846
Lin, L. I.-K. (1989). A Concordance Correlation Coefficient to Evaluate Reproducibility. Biometrics, 45(1), 255. https://doi.org/10.2307/2532051
Llorens, J., Gil, E., Llop, J., & Escolà, A. (2010). Variable rate dosing in precision viticulture: Use of electronic devices to improve application efficiency. Crop Protection, 29(3), 239-248. https://doi.org/10.1016/j.cropro.2009.12.022
Llorens, J., Gil, E., Llop, J., & Escolà, A. (2011a). Ultrasonic and LiDAR Sensors for Electronic Canopy Characterization in Vineyards: Advances to Improve Pesticide Application Methods. Sensors, 11(2), 2177-2194. https://doi.org/10.3390/s110202177
Llorens, J., Gil, E., Llop, J., & Queraltó, M. (2011b). Georeferenced LiDAR 3D Vine Plantation Map Generation. Sensors, 11(6), 6237-6256. https://doi.org/10.3390/s110606237
Lorenz, D. H., Eichorn, K. W., Bleiholder, H., Klose, U., Meier, U & Weber, E. (1994). Phänologische Entwicklungsstadien der Weinrebe (Vitis vinifera L. spp. Vinifera). (Phenological stages of grapevine (Vitis vinifera L. spp. Vinifera)). Viticultural and Enological Science 49, 66-70
Manktelow, D. W. L., & Praat, J. P. (1997). The tree-row-volume spraying system and its potential use in New Zealand. Proceedings of the New Zealand Plant Protection Conference, 50, 119-124. https://doi.org/10.30843/nzpp.1997.50.11360
Mathews, A., & Jensen, J. (2013). Visualizing and Quantifying Vineyard Canopy LAI Using an Unmanned Aerial Vehicle (UAV) Collected High Density Structure from Motion Point Cloud. Remote Sensing, 5(5), 2164-2183. https://doi.org/10.3390/rs5052164
Miranda, C., Santesteban, L. G., Escalona, J. M., De Herralde, F., Aranda, X., Nadal, M., Intrigliolo, D., Castel, J., Royo, J., & Medrano, H. (2017). Allometric relationships for estimating vegetative and reproductive biomass in grapevine (*Vitis vinifera* L.) : Allometric relations for grapevine biomass. Australian Journal of Grape and Wine Research, 23(3), 441-451. https://doi.org/10.1111/ajgw.12285
Moorthy, I., Miller, J. R., Berni, J. A. J., Zarco-Tejada, P., Hu, B., & Chen, J. (2011). Field characterization of olive (Olea europaea L.) tree crown architecture using terrestrial laser scanning

853 data. Agricultural and Forest Meteorology, 151(2), 204-214.
854 https://doi.org/10.1016/j.agrformet.2010.10.005
855 Viret, O., Siegfried, W., Wohlhauser, R. (2005). Crop adapted spraying in viticulture. Leaf volume
856 dependant pesticide dosage for a precise and ecological application. 8thworkshop on spray application
857 techniques in fruit growing, Barcelona, Spain, s. 23-24.
858 Viret, O. & Höhn, H. (2008). Application de la dose selon la méthode du TRV. Revue Suisse de
859 Viticulture, Arboriculture et Horticulture 40, 50-51.
860 Palacin, J., Palleja, T., Tresanchez, M., Sanz, R., Llorens, J., Ribes-Dasi, M., Masip, J., Arnó, J.,
861 Escolà, A., & Rosell, J. R. (2007). Real-Time Tree-Foliage Surface Estimation Using a Ground Laser
862 Scanner. IEEE Transactions on Instrumentation and Measurement, 56(4), 1377-1383.
863 https://doi.org/10.1109/TIM.2007.900126
864 Pergher, G., & Petris, R. (2008). Pesticide dose adjustment in vineyard spraying and potential for dose
865 reduction. Manuscript ALNARP 08 011. Agricultural Engineering International. CIGR Ejournal X
866 (May).
867 Poni, S., Lakso, A., Intrieri, C., Rebucci, B., & Filippetti, I. (1996). Laser scanning estimation of
868 relative light interception by canopy components in different grapevine training systems. VITIS-
869 GEILWEILERHOF, 35, 177–182.
870 Rinaldi, M, Llorens, J., & Gil, E. (2013). Electronic characterization of the phenological stages of
871 grapevine using a LiDAR sensor. Precision Agriculture Wageningen: Academic Publishers), 13, 603-
872 609.
873 Rosell, J. R., Llorens, J., Sanz, R., Arnó, J., Ribes-Dasi, M., Masip, J., Escolà, A., Camp, F.,
874 Solanelles, F., Gràcia, F., Gil, E., Val, L., Planas, S., & Palacín, J. (2009). Obtaining the three-
875 dimensional structure of tree orchards from remote 2D terrestrial LiDAR scanning. Agricultural and
876 Forest Meteorology, 149(9), 1505-1515. https://doi.org/10.1016/j.agrformet.2009.04.008
877 Rosell, J.R., & Sanz, R. (2012). A review of methods and applications of the geometric
878 characterization of tree crops in agricultural activities. Computers and Electronics in Agriculture, 81,
879 124-141. https://doi.org/10.1016/j.compag.2011.09.007
880 Rosell Polo, J. R., Sanz, R., Llorens, J., Arnó, J., Escolà, A., Ribes-Dasi, M., Masip, J., Camp, F.,
881 Gràcia, F., Solanelles, F., Pallejà, T., Planas, S., Gil, E., Val, L., & Palacín, J. (2009). A tractor-
882 mounted scanning LiDAR for the non-destructive measurement of vegetative volume and surface area
883 of tree-row plantations: A comparison with conventional destructive measurements. Biosystems
884 Engineering, 102(2), 128-134. https://doi.org/10.1016/j.biosystemseng.2008.10.009
885 Rovira-Más, F., Reid, J. F., & Zhang, Q. (2006). Stereovision data processing with 3d density maps
886 for agricultural vehicles. Transactions of the ASABE, 49,1213-1222.
887 Rüegg, J., Siegfried, W., Raisigl, U., Viret, O., Steffek, R., Reisenzein, H., & Persen, U. (2001).
888 Registration of plant protection products in EPPO countries: Current status and possible approaches to
889 harmonization. EPPO Bulletin, 31(2), 143-152. https://doi.org/10.1111/j.1365-2338.2001.tb00983.x
890 Saddem, R., Naud, O., Cazenave, P., Godary-Dejean, K., & Crestani, D. (2017). Precision spraying:
891 from map to sprayer control using model-checking. Journal of Agricultural Informatics, 8(3), 1–10.
892 Sanz, R., Palacin, J., Sisó, J., Ribes-Dasi, M., Masip, J., Arnó, J., Llorens, J., Valles, J.M., & Rosell, J.
893 (2004). Advances in the measurement of structural characteristics of plants with a LiDAR scanner.
894 International Conference on Agricultural Engineering, Leuven (Belgium). Book of Abstracts of the
895 AgEng 2004 Conference, Paper No. 27, 400–401.
896 Sanz, R., Rosell, J. R., Llorens, J., Gil, E., & Planas, S. (2013). Relationship between tree row LiDAR-
897 volume and leaf area density for fruit orchards and vineyards obtained with a LiDAR 3D Dynamic
898 Measurement System. Agricultural and Forest Meteorology, 171-172, 153-162.
899 https://doi.org/10.1016/j.agrformet.2012.11.013

Sanz, R., Llorens, J., Escolà, A., Arnó, J., Planas, S., Román, C., & Rosell-Polo, J. R. (2018). LiDAR and non-LiDAR-based canopy parameters to estimate the leaf area in fruit trees and vineyard. Agricultural and Forest Meteorology, 260-261, 229-239. https://doi.org/10.1016/j.agrformet.2018.06.017

Schultz, H. (1995). Grape canopy structure, light microclimate and photosynthesis. I. A two-dimensional model of the spatial distribution of surface area densities and leaf ages in two canopy systems. Vitis, 34, 211–215.

Schumann, A. W., & Zaman, Q. U. (2005). Software development for real-time ultrasonic mapping of tree canopy size. Computers and Electronics in Agriculture, 47(1), 25-40. https://doi.org/10.1016/j.compag.2004.10.002

Siebers, M., Edwards, E., Jimenez-Berni, J., Thomas, M., Salim, M., & Walker, R. (2018). Fast Phenomics in Vineyards: Development of GRover, the Grapevine Rover, and LiDAR for Assessing Grapevine Traits in the Field. Sensors, 18(9), 2924. https://doi.org/10.3390/s18092924

Siegfried, W., Viret, O., Huber, B., & Wohlhauser, R. (2007). Dosage of plant protection products adapted to leaf area index in viticulture. Crop Protection, 26(2), 73-82. https://doi.org/10.1016/j.cropro.2006.04.002

Solanelles, F., Escolà, A., Planas, S., Rosell, J. R., Camp, F., & Gràcia, F. (2006). An Electronic Control System for Pesticide Application Proportional to the Canopy Width of Tree Crops. Biosystems Engineering, 95(4), 473-481. https://doi.org/10.1016/j.biosystemseng.2006.08.004

Stajnko, D., Berk, P., Lešnik, M., Jejčič, V., Lakota, M., Štrancar, A., Hočevar, M., & Rakun, J. (2012). Programmable Ultrasonic Sensing System for Targeted Spraying in Orchards. Sensors, 12(11), 15500-15519. https://doi.org/10.3390/s121115500

Taylor, J., Tisseyre, B., Bramley, R., & Reid, A. (2005). A comparison of the spatial variability of vineyard yield in European and Australian production systems. Precision Agriculture, 5, 907-914.

Tisseyre, B., Mazzoni, C., & Fonta, H. (2008). Within-field temporal stability of some parameters in viticulture: Potential toward a site specific management. OENO One, 42(1), 27-39.

Torres-Sánchez, J., López-Granados, F., Borra-Serrano, I., & Peña, J. M. (2018). Assessing UAV-collected image overlap influence on computation time and digital surface model accuracy in olive orchards. Precision Agriculture, 19(1), 115-133. https://doi.org/10.1007/s11119-017-9502-0

Van der Zande, D., Hoet, W., Jonckheere, I., van Aardt, J., & Coppin, P. (2006). Influence of measurement set-up of ground-based LiDAR for derivation of tree structure. Agricultural and Forest Meteorology. 141, 147–160

Vercruysse, F., Steurbaut, W., Drieghe, S., & Dejonckheere, W. (1999). Off target ground deposits from spraying a semi-dwarf orchard. Crop Protection, 18, 565-570.

Walklate, P. J., Cross, J. V., Richardson, G. M., Murray, R. A., & Baker, D. E. (2002). IT—Information Technology and the Human Interface. Biosystems Engineering, 82(3), 253-267. https://doi.org/10.1006/bioe.2002.0082

Walklate, P. J., Cross, J.V., & Pergher, G. (2011). Support system for efficient dosage of orchard and vineyard spraying products. Computers and Electronics in Agriculture 75, 355–362

Walklate, P. J., & Cross, J. V. (2013). Regulated dose adjustment of commercial orchard spraying products. Crop Protection, 54, 65-73. https://doi.org/10.1016/j.cropro.2013.07.019

Westfall, P. H., Johnson, W. O., & Utts, J. M. (1997). A Bayesian perspective on the Bonferroni adjustment. Biometrika, 84(2), 419-427.

Wohlhauser, R. (2009). Dose rate expression in tree fruits – the need for harmonization approach from a chemical producer industry perspective. In Proceedings of the Tree Fruit Dose Adjustment Discussion Group Meeting, Wageningen, The Netherlands, September 2009.

Figures caption

Figure 1. A: Representation of the scanning procedure showing polar (distance, ρ, and angle, θ) and Cartesian (x, y, z plane) coordinate reference systems. B: Overhead view of two simulated scans along the row (x, z plane) showing projected LiDAR returns for a 1 m vine unit (0.5 m either side of the trunk). The shaded area indicates the progressive reduction in LiDAR returns across the cross-sectional area of the canopy. Legend: O - origin, LoT - Line of Trunks, D - distance between the LiDAR travel line and the LoT, $\Delta\theta$ - angular resolution of the scans, HS - height of the LiDAR above ground and HG - height of the grassed zone above the ground, ΔW - distance interval between two consecutive vertical scans and FTS - forward travel speed of tractor used to mount the LiDAR.

Figure 2. View (y, z plane) of a LiDAR point cloud corresponding to a vine unit at BBCH 14 to illustrate the points deleted in the automated filtration step (blue) and points retained (red) to calculate canopy dimensions. The four filter functions applied to this LiDAR point cloud (in dotted lines) are (1) inter-row ground filter based on angle (δ), (2) filtering of adjacent rows based on the distance (D), (3) grassed zone filtering, based on the height of the grassed zone (HG) and (4) near point filtering.

Figure 3. Examples of the vertical distribution of the intercepted points in the 3D LiDAR point clouds on one vine unit at three phenological stages illustrating how the BPCC algorithm filters and classifies the point cloud into different zones (non-vine ground vegetation in white, trunk zone in red, canopy zone in green and trellis wire in blue). A = BBCH 14 (early season); B = BBCH 57 (mid-season) and C = BBCH 76 (mid-late season). A and B have three distinct zones (trunk – canopy – trellis wire), while C exhibits only two zones as the trellis wire is covered by the canopy. The horizontal lines (in yellow) represent the σ-based thresholds (β_H: with $\sigma = 2$ for A and B, and 3 for C) that were used in the BPCC to define the canopy zone. The dotted line indicates the threshold used for the grassed zone filter (HG) that changes as the under-vine vegetation grows. The black line represents the distribution of points in the canopy zone only.

Figure 4. Examples of the LiDAR point clouds on one vine unit seen from the inter-row to illustrate how the proposed BPCC filtering and classification algorithm defines the canopy height (VH) and the undervine grass height (HG) at different phenological stages of the season. (A, B and C: same stages as Fig. 3). The horizontal lines (in yellow) represent the σ-based thresholds (β_H: with $\sigma = 2$ for A and B, and 3 for C) that were used in the BPCC to define the canopy zone at each stage. The dashed line indicates the derived threshold for the grassed zone filter (HG) that changes as the under vine vegetation grows. For comparison, the canopy height derived from the PROTOLIDAR method is shown in B illustrating the effect of the trellis wire on VH estimates with PROTOLIDAR with larger canopies.

Figure 5. Examples of cross-sections ('scans') of LiDAR points for one vine unit at three different phenological stages (same vine and stages as shown in Fig. 4), illustrating how the proposed BPCC filtering and classification algorithm and the PROTOLIDAR method define canopy width (VW). The vertical lines represent the extremes of canopy width from both approaches. The BPCC has a 5% threshold to estimate the half-row width (solid line) and the distal extreme is estimated assuming symmetry (dashed lines). The PROTOLIDAR derives width directly from the LiDAR returns and underestimates canopy width in larger canopies (B and C) relative to the BPCC.

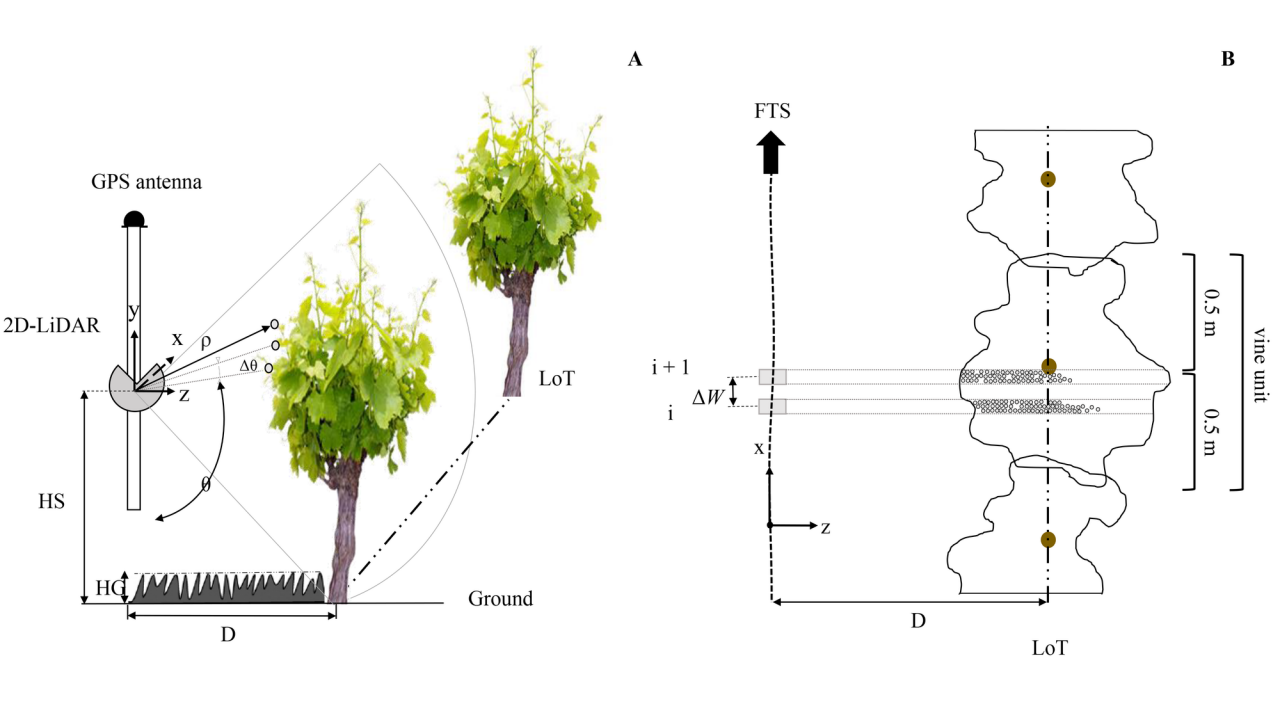
A
GPS antenna
2D-LiDAR
y
x
ρ
Δθ
z
θ
HS
HC
D
LoT
Ground
B
FTS
i + 1
i
ΔW
x
z
D
LoT
0.5 m
0.5 m
vine unit

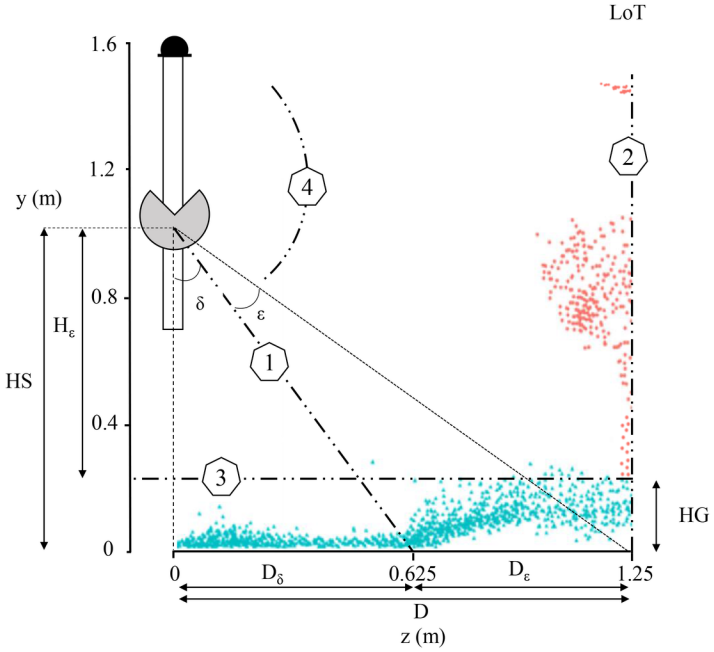
LoT
1.6
1.2
0.8
0.4
0
y (m)
HS
H_ε
δ
ε
1
2
3
4
HG
0
D_δ
0.625
D_ε
1.25
D
z (m)

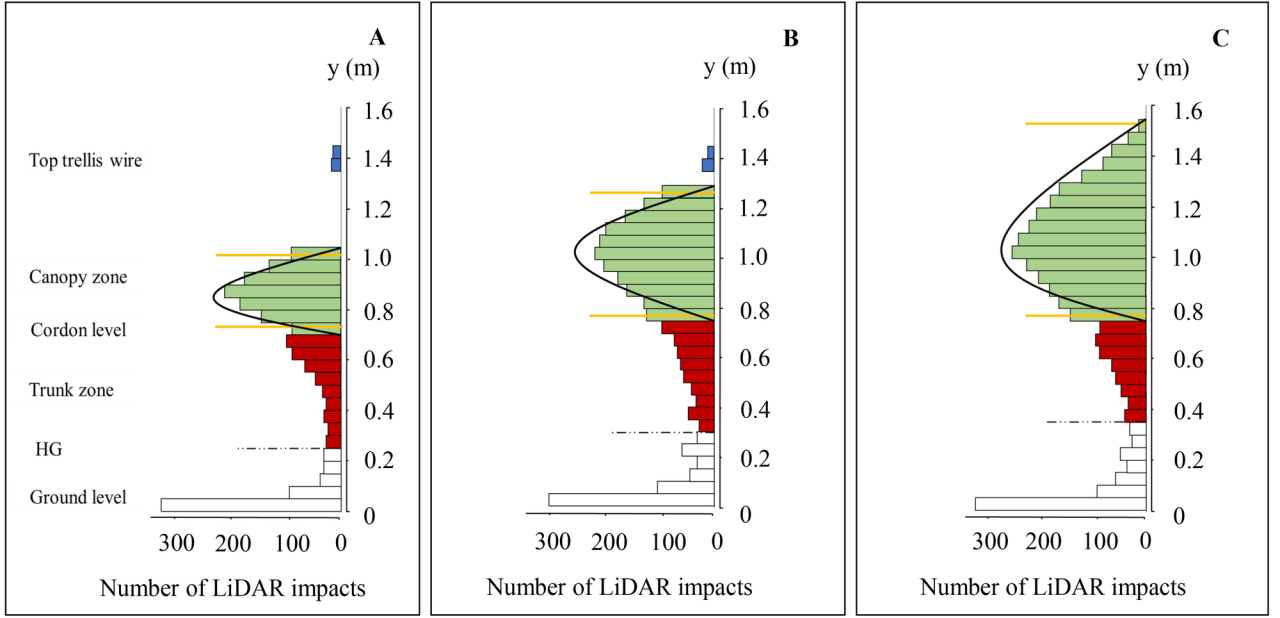
A
y (m)
1.6
1.4
1.2
1.0
0.8
0.6
0.4
0.2
0
Top trellis wire
Canopy zone
Cordon level
Trunk zone
HG
Ground level
300 200 100 0
Number of LiDAR impacts
B
y (m)
300 200 100 0
Number of LiDAR impacts
C
y (m)
300 200 100 0
Number of LiDAR impacts

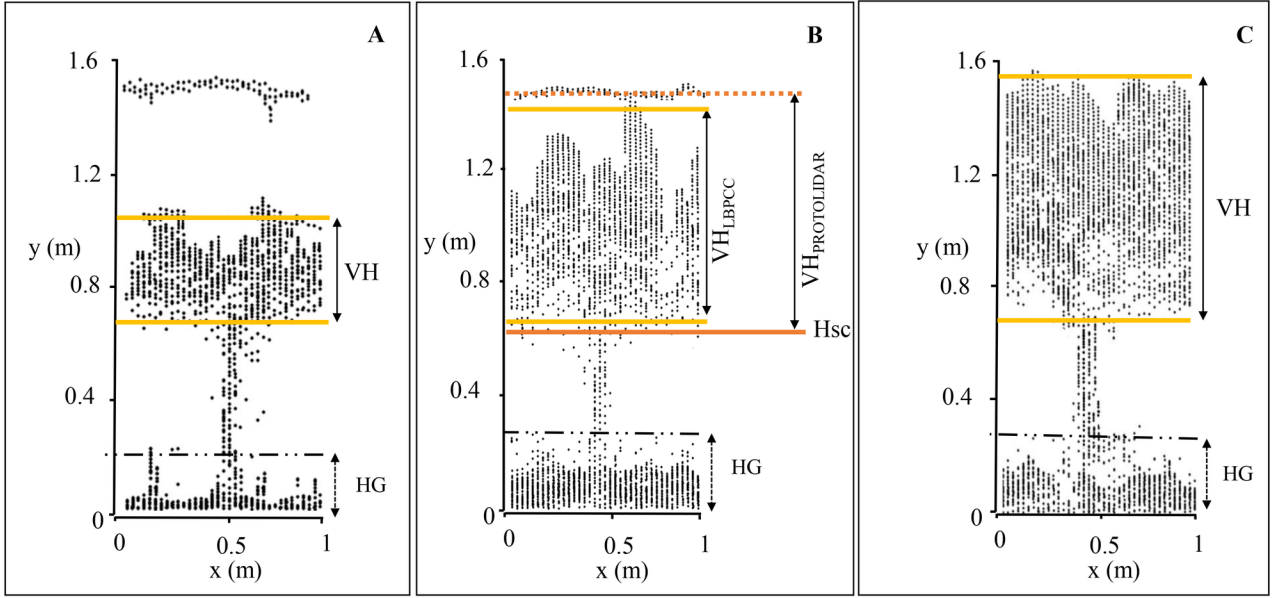
A
B
C
1.6
1.2
0.8
0.4
0
y (m)
x (m)
0
0.5
1
VH
HG
VH_LBPCC
VH_PROTOLIDAR
Hsc

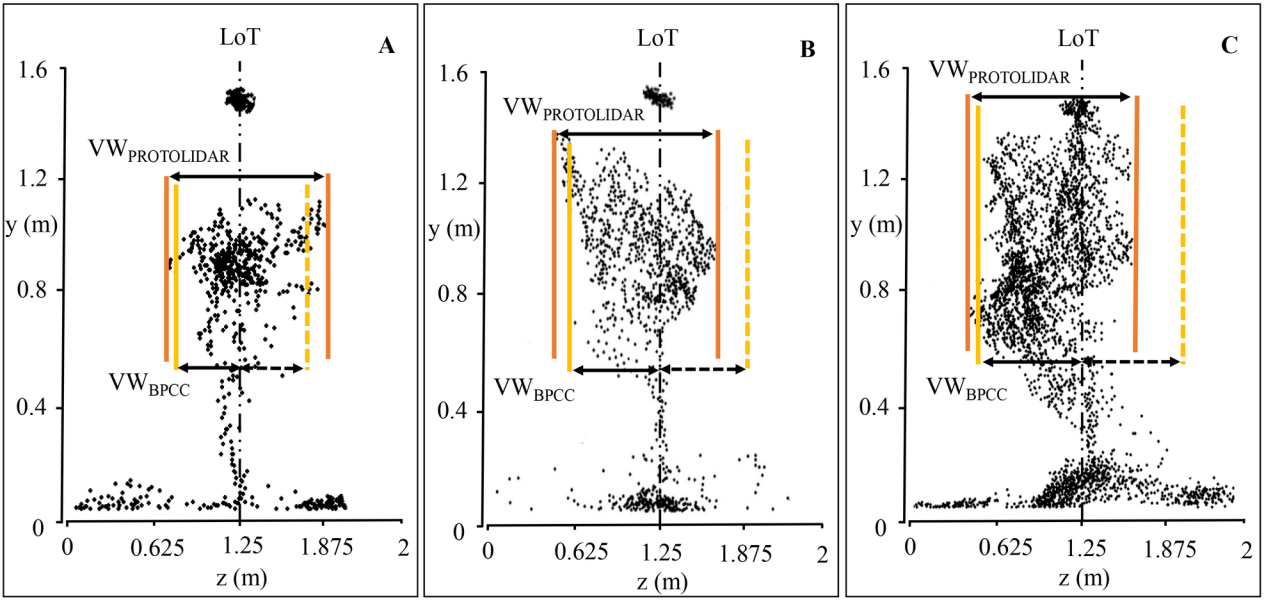
A
B
C
LoT
VW PROTOLIDAR
VW BPCC
y (m)
z (m)
1.6
1.2
0.8
0.4
0
0.625
1.25
1.875
2

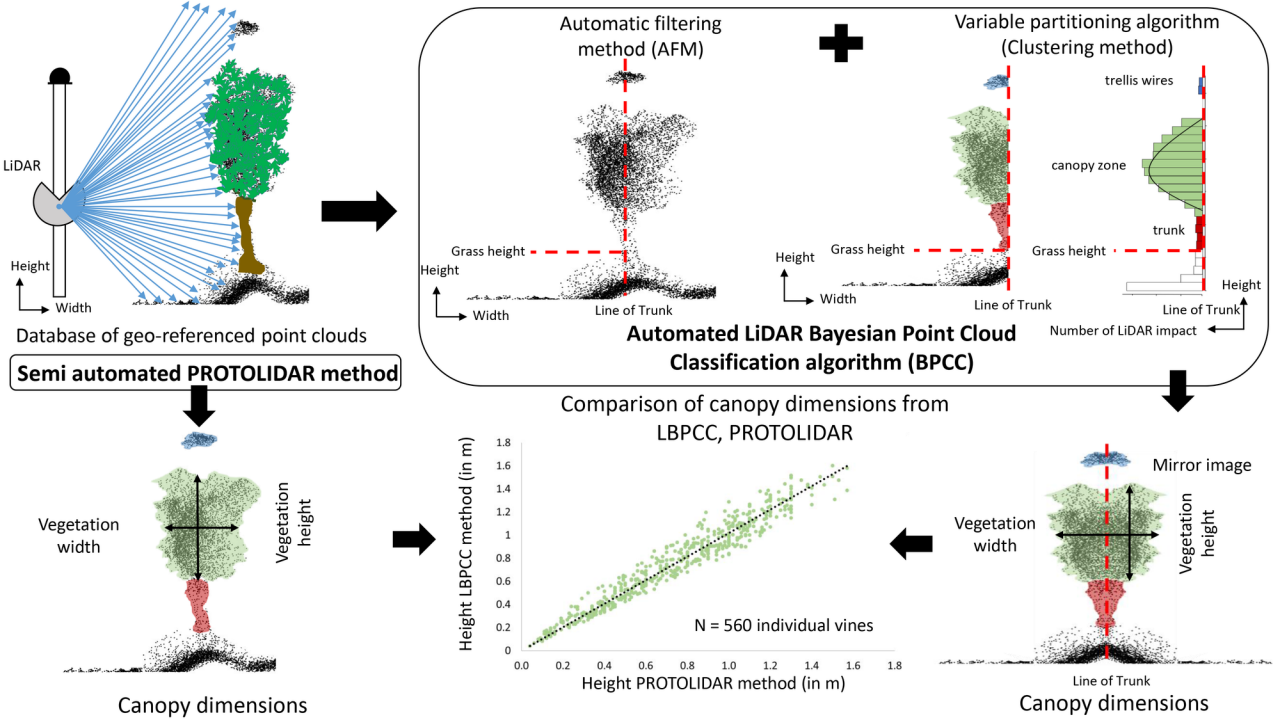
LiDAR
Height
Width
Database of geo-referenced point clouds
Automatic filtering method (AFM)
Grass height
Height
Width
Line of Trunk
Variable partitioning algorithm (Clustering method)
trellis wires
canopy zone
trunk
Grass height
Height
Width
Line of Trunk
Number of LiDAR impact
Automated LiDAR Bayesian Point Cloud Classification algorithm (BPCC)
Semi automated PROTOLIDAR method
Vegetation width
Vegetation height
Canopy dimensions
Comparison of canopy dimensions from LBPCC, PROTOLIDAR
Height LBPCC method (in m)
Height PROTOLIDAR method (in m)
N = 560 individual vines
Mirror image
Vegetation width
Vegetation height
Line of Trunk
Canopy dimensions